JOURNAL OF MATERIALS SCIENCE 29 (1994) 939–942

Morphology of (Ru–Ti–Sn) mixed-oxide coatings

S. PUSHPAVANAM, K. C. NARASIMHAM
Central Electrochemical Research Institute Karaikudi, 623006, India

Noble-metal-oxide-based coatings have successfully replaced many of the conventional anode materials in industrial electrochemical processes. The performance characteristics of these mixed-oxide electrodes have been found to be improved by the inclusion of non-noble-metal-oxide components. Of these, the addition of SnO_2 to RuO_2–TiO_2 has attracted much attention. In the present paper, the morphology change imparted by gradual replacement of TiO_2 by SnO_2 from the RuO_2–TiO_2 (30/70) coatings is reported. Scanning electron microscopic examination and porosity determination reveal that significant modifications take place in the surface structure, and the surface layer tends to become compact at SnO_2 concentration above 30 mol% SnO_2.

1. Introduction

Mixed-oxide coatings of the dimensionally stable anode (DSA) type consist of (apart from noble-metal and valve-metal oxides) various non-noble-metal oxides, which impart certain desirable characteristics, such as stability and selectivity [1, 2]. The inclusion of tin oxide, though patented in 1973 [3], has only been the subject of some basic studies recently [4–8]. In previous papers, the structural variations of the ternary (Ru–Ti–Sn) mixed oxides of various compositions were reported [5, 6]. The present work relates to the changes observed in the morphology of these coatings as a function of the ratio of TiO_2 to SnO_2 in the mixed oxide, while the RuO_2 content is kept constant at 30 mol %.

2. Experimental procedure

Mixed-oxide electrodes were prepared, as described in [5, 6], on pre-treated titanium and nickel strips.

The texture of the mixed-oxide-coated titanium surfaces were examined by scanning electron microscopy (SEM, JEOL, Japan).

The porosities of the oxide-coated samples at different thicknesses were compared by measurement of the rate of corrosion of the substrate using the electrodes prepared on a nickel base.

The corrosion measurement was carried out in a 0.5 M sulphuric acid solution using a H-type cell fitted with a platinum counter electrode. The instrumentation consisted of a potentiogalvanoscan (Wenking, PGS 81) in combination with a logarithmic-output current sink (Wenking, MLS 81) and an $(x-y)/t$-recorder (Rikadenki). The electrolyte was deaerated with purified nitrogen before each experiment, and the working electrode was allowed 60 min to attain a steady potential after which the potential was scanned at the rate of 0.1 $mV\,s^{-1}$.

3. Results

SEM micrographs of the oxide coatings are presented in Fig. 1. The highly cracked configuration of RuO_2–TiO_2 seems to be retained up to 20 mol % tin oxide (Fig. 1a–b). There is then a steady increase in the number of islands with a simultaneous decrease in the cross-sectional dimension of the cracks. The RuO_2–SnO_2 (30/70) shown in Fig. 1f has practically minimum breaks in the surface continuity. Fig. 1c to f indicate the gradual change in the surface morphology – from a honeycomb structure to a fairly compact and smooth surface, having only microcracks and pores.

From the potentiodynamic corrosion curves of the electrodes coated with the series of oxide compositions of various loadings, the corrosion current, (I_{cor}), was obtained. The variation of I_{cor} with the oxide loadings of the coatings is shown in Fig. 2. The rate of corrosion initially decreased and after a certain thickness it became constant. The amount of the oxide loading after which I_{cor} is almost constant is given in Table I. This critical loading can be seen to be higher for RuO_2–TiO_2 than for the other compositions containing SnO_2.

Fig. 3 shows I_{cor} values, at a constant loading of 1.6 $mg\,cm^{-2}$, as a function of the concentration of SnO_2. The corrosion rate drops only gradually at lower additions of SnO_2, while the decrease is significant above 30 mol % SnO_2.

4. Discussion

4.1. Surface examination

The surface structure of the thermally produced RuO_2-based coatings depends on several factors, such as the concentration of the coating solution, the nature of the solvent, the technique used to apply the

0022–2461

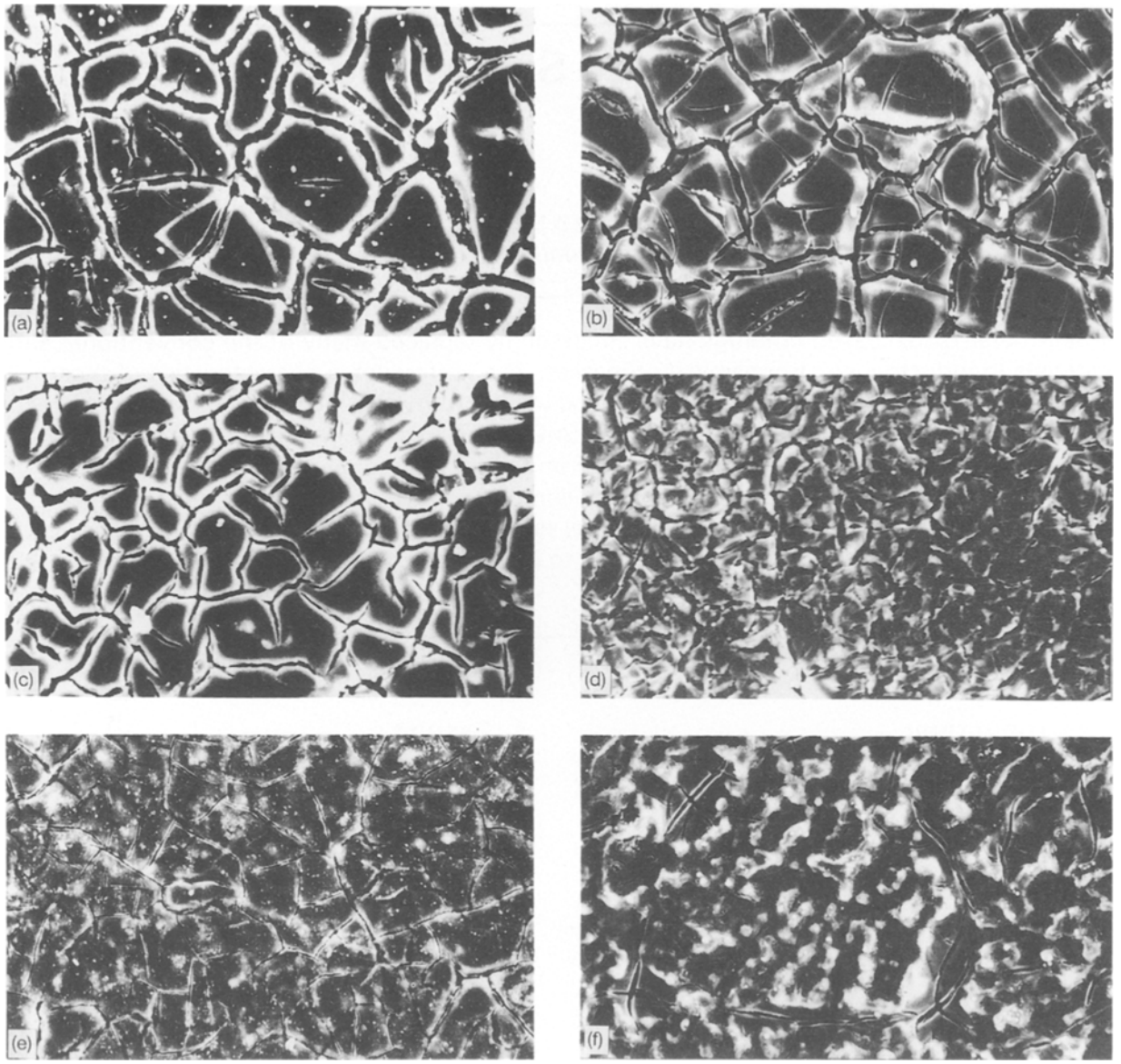

Figure 1 SEM micrographs of the mixed-oxide films (RuO_2–TiO_2–SnO_2) for the following molar percentage ratios: (a) 30/70/0, (b) 30/50/20, (c) 30/40/30, (d) 30/20/50, (e) 30/10/60, and (f) 30/0/70.

coating, the temperature, the heating rate and atmosphere and the nature of the substrate [9]. Generally, these coatings have a "cracked-mud" morphology [5, 10–12]. The surfaces shown in Fig. 1 for coatings with 0–30 mol % SnO_2 reveal the qualitative similarities with the surface usually observed. This type of structure is due to solvent evaporation, as well as due to the difference in the thermal coefficient of expansion between the substrate and the coating, which induces mechanical stresses that are not compensated for by the rigidity of the oxide layer [13, 14].

As the tin-oxide content increases further, the crack width narrows, bringing the islands close together. This is attributed to the decreasing crystallinity, as observed from the X-ray diffraction (XRD) analysis [6], at decreasing ratios of TiO_2 to SnO_2 in the mixed oxides. Increasing substitution of TiO_2 with SnO_2 reduces the grain size, with a simultaneous tendency towards compaction. The amorphous nature of the tin oxide (as indicated from its ability to form transparent film [15]) enables it to provide a better distribution and coverage of the surface. The physical properties of the constituent oxides, as shown in Table II [16–18], help in understanding this type of structure development. It will be observed that: (i) RuO_2 and SnO_2 have almost equal specific gravities whereas those of RuO_2 and TiO_2 differ widely; and (ii) the coefficient of linear expansion for SnO_2 is almost half that for TiO_2, and the cubical expansion for SnO_2 is one-third of that for TiO_2. Moreover, SnO_2 and RuO_2 have almost the same cubical expansion. The size of the islands and the width and depth of the crevices decrease significantly above 30 mol % SnO_2. A similar observation has been reported in the case of the binary RuO_2–TiO_2 system, wherein the concentration of the RuO_2 determines the microprofile [19]. The fairly smooth and compact texture of the binary RuO_2–SnO_2 (Fig. 1f) was also observed previously [20]. Usually the size of the pores and cracks decrease with increasing thickness. But, under constant loading, the thickness of the mixed-oxide layer decreases with increasing percentages of tin oxide and the surface structure still tends to be-

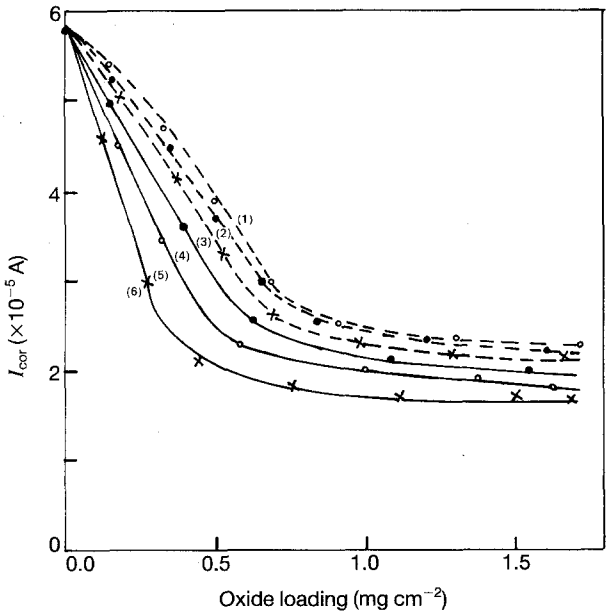

Figure 2 The effect of the oxide loading (mg cm^{-2}) of the mixed-oxide coatings on the corrosion rate for an electrolyte of 0.5 M H_2SO_4 and a temperature of 303 K. The following compositions (in mol %) of RuO_2–TiO_2–SnO_2 were used: (1) (30/70/0, (2) (30/50/20), (3) (30/40/30), (4) (30/30/40), (5) (30/10/60), and (6) (30/0/70).

TABLE I Effect of the coating composition on the critical loading

Electrode $RuO_2/TiO_2/SnO_2$ (mol %)	Limiting oxide loading (mg cm^{-2})
30/70/0	0.78
30/50/20	0.75
30/40/30	0.68
30/30/40	0.65
30/10/60	0.54
30/0/70	0.45
Nickel	–

come compact. This leads to the conclusion that the modifications in the surface structure is definitely attributable to the presence of tin oxide and its microcrystallinity.

4.2. Porosity

Usually, the porosity of metallic coatings on metal substrates are evaluated by: (a) a microscopic method, (b) a ferroxyl test (for steel substrates), or (c) corrosion-rate measurements [21–23]. In the present investigation, the last method was adopted. To suit the analysis, a nickel substrate was chosen, because of the complexity of titanium corrosion. Employment of a nickel substrate for this type of study has already been reported [19, 23].

The variation in the corrosion potential and current of the substrate with respect to the porosity of the overlying coating has been utilized in a study of electroplating [24] as well as for oxide coatings [25]. As it is not the aim of this study to evaluate the

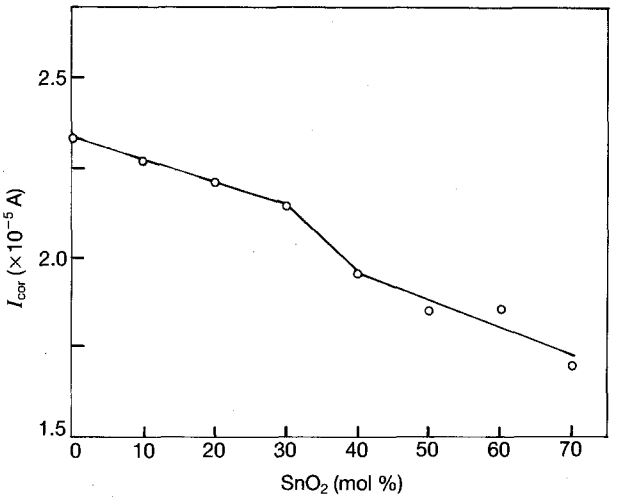

Figure 3 The change in the corrosion rate as a function of the SnO_2 content at an oxide loading of 1.6 mg cm^{-2}.

TABLE II Some physical properties of RuO_2, TiO_2 and SnO_2

Sample number	Property	RuO_2 [16]	TiO_2 [17]	SnO_2 [18]
1	Specific gravity	7.05	4.25	6.6–6.9
2	Linear expansion ($\times 10^{-6}$) (273–319 K)			
	Along *a*-axis	9.0	9.19	4.0
	Along *c*-axis	1.7[a]	7.14	4.8
3	Cubical expansion ($\times 10^{-5}$)	1.6	3.2	1.3–1.6

[a]Contraction.

absolute values of the porosities, the relative corrosion rate as a function of the oxide loading and the composition was evaluated.

Penetration of the electrolyte through the coating had been previously observed, by observing the rate of change of the stationary potential [19], and also by spectroscopy [26]. Thus, the corrosion-current values are definite indications of the extent of through-porosities of the coatings. The sizes of the pores and cracks attain a constant minimum above a limiting value of the thickness, as revealed by Fig. 2 where I_{cor} is constant after a certain loading. This limiting loading indicates the minimum thickness required to produce a coating of a composition with practically no through-pores and cracks. This critical thickness varies with the composition of the coating, as shown in Table I, where other parameters were maintained at constant values throughout. An increase in the tin-oxide content decreases the corrosion rate; in other words, the electrolyte diffusion through the coating and its attack on the substrate is gradually inhibited (Fig. 3). The observations in the SEM micrographs corraborate the results of the porosity changes with the SnO_2 content. Since the solvent and the substrate are uniformly the same for all the types of the oxide layers examined, the determining factors in the development of the observed morphologies must be not

only the glass-forming nature of the tin oxide but also a probable change in the crystallization process at different ratios of titanium and tin oxide.

5. Conclusion

In the Ru–Ti–Sn mixed-oxide coatings, the morphology and porosity of the coating is largely controlled by the ratio of TiO_2 to SnO_2 when the RuO_2 component is kept constant. The higher the tin-oxide content is, the more compact is the layer.

Acknowledgement

The authors wish to express their gratitude to Professor S. K. Rangarajan, the Director of the Central Electrochemical Research Institute, Karaikudi, for his support and encouragement in publishing this work.

References

1. V. De NORA, Extd. Abst. Electrochemical Society Meeting, Vol. 78-1 (1978) Abstract Number 458.
2. A. NIDOLA, in "Electrodes of Conductive Metallic Oxides", Part B edited by S. Trasatti (Elsevier, Amsterdam, 1980) p. 627.
3. K. J. O'LEARY, US Patent 3 776 834 (1973).
4. A. BANDI, I. VARTIRUS, A. MIHELIS and C. HAINAROSIE, *J. Electroanal. Chem* **157** (1983) 241.
5. S. PUSHPAVANAM, K. C. NARASIMHAM and K. I. VASU, *Bull.Electrochem.* **4** (1988) 979.
6. *Idem.* to be published.
7. J. F. C. BOODTS and S. TRASATTI, *J. Electrochem. Soc.* **137** (1990) 3874.
8. A. I. ONUCHUKWU and S. TRASATTI, *J. Appl. Electrochem.* **21** (1991) 858.
9. S. TRASATTI and G. LODI, in "Electrodes of conductive Metallic oxides" Part A, edited by S. Trasatti (Elsevier, Amsterdam, 1980) p. 301.
10. S. PIZZINI, G. BUZZANCA, C. MARI, L. ROSSI and S. TORCHIO, *Mater. Res. Bull.* **7** (1972) 1449.
11. W. A. GERRARD and C. H. STEELE, *J. Appl. Electrochem.* **8** (1978) 417.
12. G. BARREL, J. GUITTON, C. MONTELLA and F. VERGARA, *Surf. Technol.* **6** (1977) 39.
13. K. J. O'LEARY and T. J. NAVIN, in Proceedings of the Chlorine Bicentennial Symposium, edited by T. C. Jeffrey, P. A. Dunna and H. S. Holden, (Electrochemical Society, Princeton, New Jersey, 1974) p. 174.
14. S. TRASATTI and W. E. O'GRADY, in "Advances in electrochemistry and electrochemical engineering" Vol. 12, edited by H. Gerisher and C. W. Tobias, (Wiley, New York, 1981) p. 177.
15. H. KIM and H. A. LAITINEN, *J. Electrochem. Soc.* **122** (1975) 53.
16. J. M. FLETCHER, W. E. GARDNER, B. E. GREENFIELD, M. J. HOLDAWAY and M. H. RAND, *J. Chem. Soc. A* (1968) 653.
17. J. W. MELLOR, in "Comprehensive treatise on inorganic and theoretical chemistry" Vol. VII (Longmans, UK, 1947) p. 37.
18. C. L. MANTELL, in "Tin and its mining, production and technology" (Hartner, 1970) p. 412.
19. Yu. B. MAKARYCHEV, E. K. SPASSKAYA, S. D. KHODKEVICH and L. M. YAKIMENKO, *Sov. Electrochem.* **12** (1976) 921.
20. C. IWAKURA and K. SAKAMOTO, *J. Electrochem. Soc.* **132** (1985) 2420.
21. "Metal finishing, guide book and directory", (Metals and Plastics. Publishing Inc., New Jersey, 1986) p. 598.
22. R. BABOIN, in "Electrochemical techniques for corrosion" (NACE, Texas, 1978).
23. M. CLARKE, in "Properties of electrodeposits", edited by R. Sard, H. Leidheiser and F. Ogburn (Electrochemical Society, Princeton, NJ, 1975) p. 122.
24. K. S. RAJAM, and S. R. RAJAGOPALAN, in Proceedings of the Tenth International Congress on Metallic Corrosion, Vol. II, (Oxford and IBH, New Delhi, 1987) p. 1243.
25. J. PRABHAKAR RATHINARAJ, S. KULANDAISAMY, S. C. CHOCKALINGAM, S. VISWANATHAN and K. S. RAJAGOPALAN, in Proceedings of the Symposium on Advanced Electrochemicals, Karaikudi, India (1984), p. 21.
26. C. IWAKURA, M. INAI, M. MANABE and H. TAMURA, *Denki Kagaku* **48** (1980) 91.

Received 9 September 1992
and accepted 9 September 1993